Res. Rep. Fac. Eng. Mie Univ., Vol. 22, pp. 79−94 (1997)

Original Paper

Structural Behavior and Characteristics of Concrete-Filled Tubular Frames

Jun KAWAGUCHI, Shosuke MORINO, Toshikazu SUGIMOTO† and Junya SHIRAI
(Department of Architecture)

(Received September 12, 1997)

ABSTRACT

In order to clarify the elasto-plastic behavior of the frame consisting of concrete-filled steel tubular (CFT) columns and H-shaped steel beams under seismic loading, portal frame specimens were tested under constant vertical loads on columns and alternately repeated horizontal load. Experimental parameters were: axial load ratio, and width-to-thickness ratio, and yield mode. D_S factors were calculated from the load-deflection curves of all specimens. It was observed that all specimens showed fairly stable hysteresis loops, and the earthquake resistant capacity of the CFT frame was better than the similar steel frame.

Keywords: CFT, portal frame, elasto-plastic behavior, structural characteristic factor

1. Introduction

CFT frames consist of concrete-filled steel tubular (CFT) columns and pure steel beams, and they have become very popular these days, since it has been verified by many investigations since the 1970's that CFT columns have more benefit compared with ordinary steel columns, that is, CFT columns have more load carrying capacity than hollow steel tubular columns due to the interactive effects between steel and concrete; the confining effect of the steel tube on the concrete, and the restraining effect of filled-concrete on the local buckling of the steel tube. The behavior of the beam-to-column connections, including new types of diaphragm system, were also investigated experimentally. However, very few frame tests have been done. *Matsui*[1] carried out tests of the CFT frames of the column yielding type with changing width-to-thickness ratio of the column tube, diaphragm type, and loading histories. He concluded that the CFT frame showed excellent horizontal load carrying capacity and the limit value of the width-to-thickness ratio of the CFT column could be relaxed to about 1.5 times that for hollow tubes due to the effects of filled-concrete on the local buckling strength and post buckling behavior of the tube. *First two authors*[2] carried out an experimental study on the elasto-plastic behavior of three-dimensional subassemblages consisting of CFT columns and steel beams, and concluded that specimens which yielded in connection showed more energy dissipation capacity than specimens of yielding in columns, and three-dimensional loading caused strength deterioration only in specimens of yielding in columns. This paper presents the test results of CFT portal frames, which were conducted to clarify the elasto-plastic behavior of CFT frames, and obtain D_S values for the efficient design practice.

† General Building Research Corporation

2. Experiment

2.1 Outline of Tests

Tested in this research were the portal frame specimens consisting of the concrete-filled steel square tubular (CFT) columns and a pure steel beam, subjected to the constant vertical load P on the columns and the alternately repeated horizontal load H, shown in Fig. 1. Experimental parameters included the width-to-thickness ratio of the column tube (D/t = 21, 39 and 54), yield mode (column-yielding type and panel-yielding type), and applied axial load ratio relative to the yield load of the column (N/N_y = 0.15 and 0.3), where $N = P/2$, $N_y = A_cF_c + A_s\sigma_y$, and A_c and A_s denote the cross-sectional areas of concrete and steel, respectively, and F_c and σ_y the cylinder strength of concrete and yield stress of steel, respectively. These values of width-to-thickness ratio correspond to FA, FB and FD ranks according to *BCJ Requirements*[3]. The specimen identification and the experimental parameters are shown in Table 1. The first and the last two digits of the specimen name indicate the vertical load ratio and the width-to-thickness ratio, respectively, and the letters SCC and SCP denote the column-yielding and panel-yielding specimens, respectively.

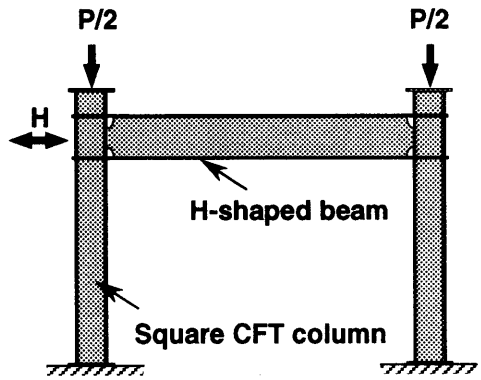

Fig. 1 Schematic view of test

Table 1 Specimens and parameters

Specimens	B/t	Failing type	N/Ny (%)
21SCC15	21	column	15
21SCC30	21	column	30
21SCP15	21	connection	15
21SCP30	21	connection	30
39SCC15	39	column	15
39SCC30	39	column	30
54SCC15	54	column	15
54SCC15	54	column	30

2.2 Shape and Dimensions of Specimens

Figure 2 shows the shape and dimensions of a specimen, which consists of CFT columns (□-125x125xt_c) and a built-up H-shaped steel beam. A total of eight specimens were prepared with three different width-to-thickness ratio of the column tubes. The beam length (distance between column center lines) was 1,500 *mm*, and the column height (distance between the beam center line and the surface of the column base stub) was 1,000 *mm*. The beam was connected by welding to the columns with through-type diaphragms which had holes for concrete casting. The beam was extended outside the column to apply the horizontal load, and it was also extended at the other side to

make the restraining condition on the beam-to-column connection the same as the loading side, except for the specimens with D/t = 21 which were tested at the earliest time. The columns were also extended upward from the beam to apply the vertical load, and this portion was made of the same steel tube as used for the tested portion. The thickness of the diaphragm plate was the same as that of the beam flange. The specimens were designed to yield in column (SCC) or in connection panel (SCP), and the beam was designed to behave elastically until the end of the test. The thickness of steel tube used for the connection panel of the column-yielding specimen is the same as that of the column. The specimens of the panel-yielding type were prepared only for the specimens with D/t = 21, where the thickness of the column tube was 6 mm, and that of the panel tube was 3.2 mm. It is almost impossible to proportion the panel tube for the column-yielding specimens with D/t = 39 or 54 . Column tubes were connected to the diaphragm plates by butt welding except for the specimens with D/t = 21, in which fillet welding was accidentally used. At the column base, the column tube was inserted into a base stub consisting of an H-150x260x12x16, and fillet welding was used at the connection between the column tube and upper and lower flanges of the base stub, as shown in the figure. Table 2 shows the measured dimensions of the specimens. The definitions of symbols used in Table 2 are given in Fig. 3.

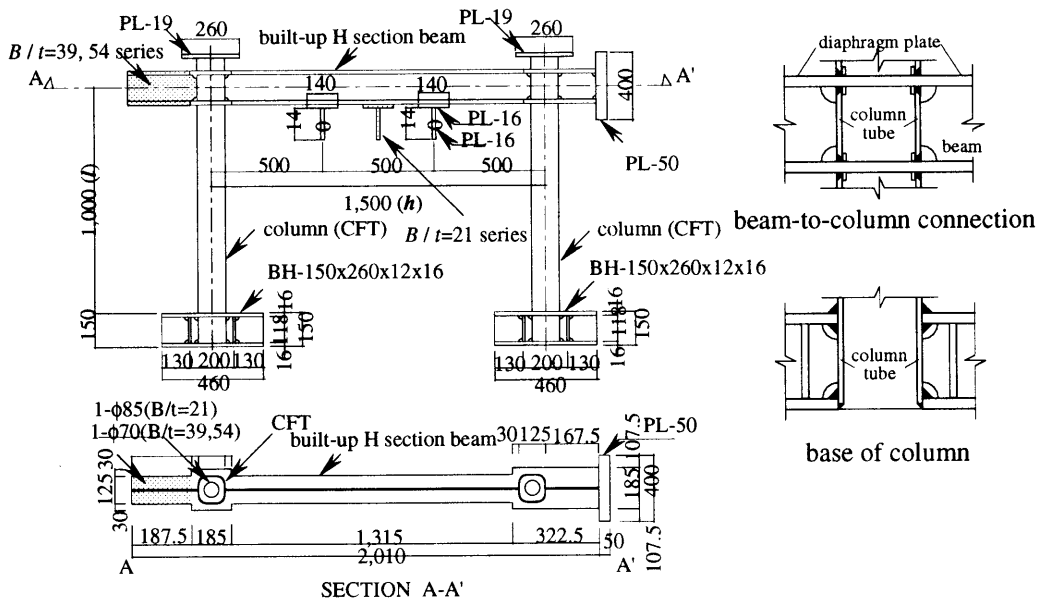

Fig. 2 Shape of specimen

2.3 Materials

The column tubes of the specimens with D/t = 21 and 39 were cold formed square sections made of STKR400 grade steel as per Japanese Industrial Standards, and Those of the specimens with D/t = 54 were made by seaming two cold formed channels of SS400 grade steel by butt welding. The beams were made of SS400 grade steel. Any parts of the specimen were not annealed to remove the residual stresses. The stress-strain relations of steel obtained from the tests of coupons taken from the flat portion of the column tube and the plates used for the beam fabrication are shown in Fig. 4, and the mechanical properties are given in Table 3. Two kinds of □-125x125x3.2, marked A and B in Table 3, were used; the portions of the specimens fabricated by using these materials are indicated in Table 2. The mixture of concrete and the properties of concrete obtained from the cylinder tests are shown in Tables 4 and 5.

2.4 Procedure of the Test

Figure 5 shows the test setup. First, a constant vertical load on the column was applied by a 980 *kN* hydraulic jack through the upper loading beam. Then, a cyclic horizontal load was applied by a 490 *kN* horizontal hydraulic jack connected to the lower base beam. A 490 *kN* servo pulser was set at the column top to adjust the horizontal displacement at the column top to be zero, *i.e.*, the original position. The out-of-plane deformation of the beam was prevented at two points (at the center in the case of the specimens with D/t = 21) by the caterpillar type deflection stopper.

Table 2 Measured dimensions (*mm*)

specimens	D_c	t_c	d_p	D_p	t_p	D_b	B_b	t_{bf}	t_{bw}	h	l
21SCC15	125.35	5.80	122.92	125.15	5.80	125.92	148.40	24.84	15.00	997.9	1499
21SCC30	125.23	5.80	124.61	125.15	5.80	125.52	149.20	24.57	15.00	999.1	1499
21SCP21	125.44	5.80	125.32	125.32	2.99B	125.59	148.90	24.80	15.00	997.5	1500
21SCP30	125.60	5.80	123.55	125.49	2.99B	125.67	149.10	24.81	15.00	996.4	1500
39SCC15	125.57	3.03A	141.33	124.11	3.03A	124.97	150.12	8.79	5.84	1002.6	1499
39SCC30	125.57	3.03A	140.65	123.68	3.03A	126.17	149.49	8.84	5.84	1003.1	1500
54SCC15	126.32	2.29	143.83	124.84	2.29	124.98	150.52	5.98	4.29	1002.1	1498
54SCC30	125.83	2.29	144.54	124.29	2.29	125.38	149.73	5.90	4.29	1003.2	1498

D_c: width/depth of column tube D_p : width/depth of steel connection tube D_b :depth of beam
t_c : thickness of column panel t_p: thickness of steel connection panel B_b : width of beam
d_p : height of connection panel (between center of diaphragms) h : column length(see Fig. 3) l : beam length(see Fig. 3) t_{bf}: flange thickness of beam t_{bw}: web thickness of beam

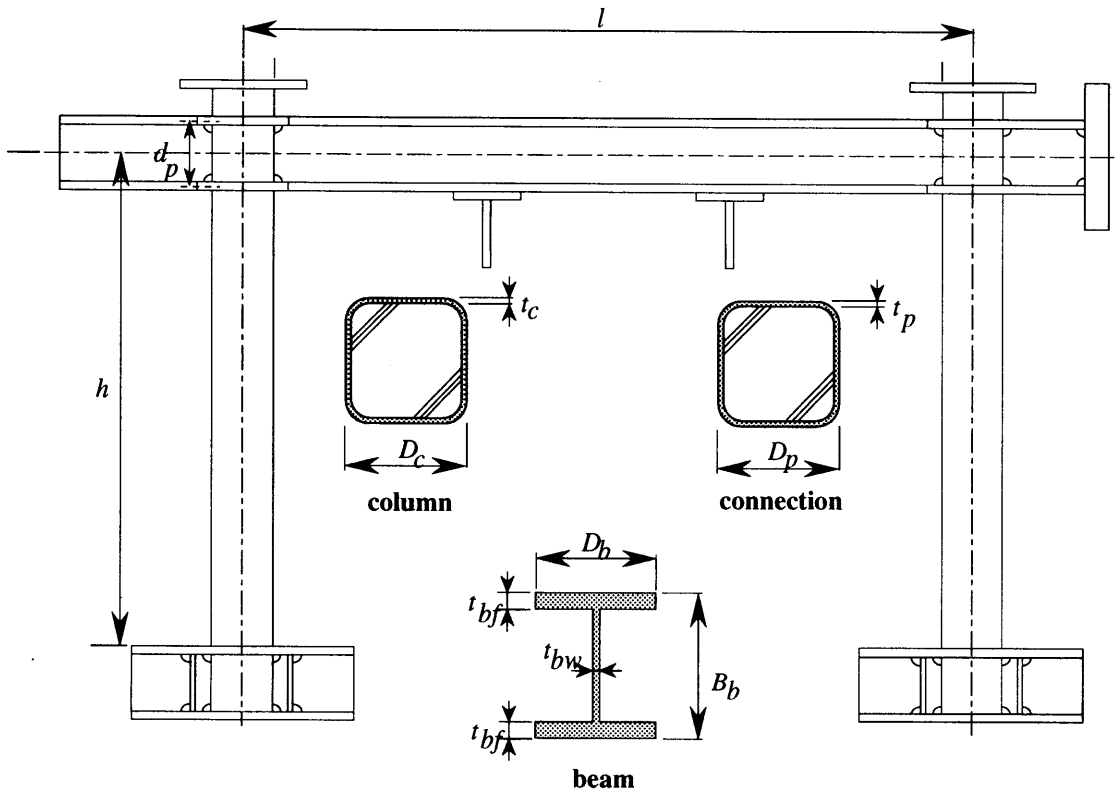

Fig. 3 Dimentions of specimen

The relative horizontal displacement Δ between the center of the connection panel and the base beam was measured by two displacement meters, as shown in Fig. 6. The longitudinal strains at several points on the columns, and three-directional strains of the connection panel were measured by uniaxial- and rosette-type three-directional wire strain gauges, as shown in Fig. 7.

Figure 8 shows the loading rule used in the tests. The first cycle of loading was applied by controlling the amplitude of the column chord rotation angle equal to ± 0.5/100 *radian*, where chord rotation angle is the relative horizontal displacement Δ divided by the column length h. The second and the third cycle were applied at the amplitude equal to ± 1/100 *radian*. From the forth cycle, two cycles of loading were applied at each amplitude, which was increased by ± 1/100 *radian*.

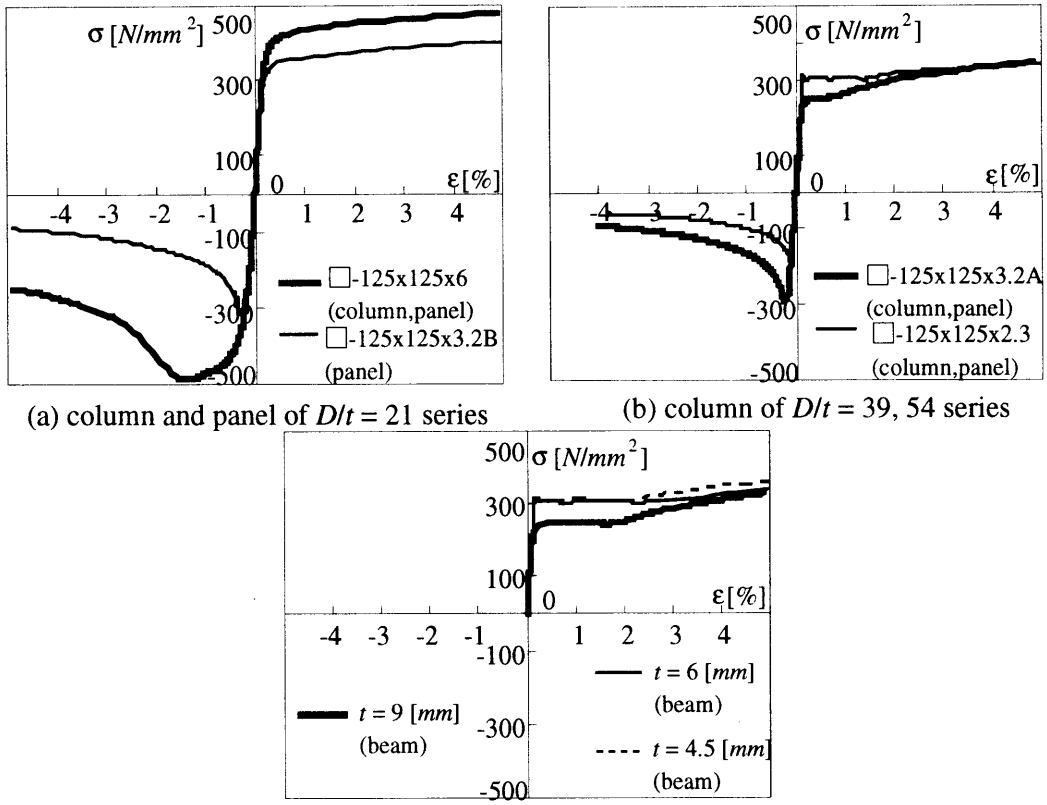

(a) column and panel of D/t = 21 series

(b) column of D/t = 39, 54 series

(c) beam

Fig. 4 Stress-strain curves

Table 3 Mechanical properties of steel

Test piece	σ_y [N/mm²]	σ_u [N/mm²]	ε [%]	E_s [N/mm²]	$\varepsilon_{st}/\varepsilon_y$	E_{st}/E_s	σ_c [N/mm²]
□-125x125x**2.3** (column, panel)	328.19	382.30	22.92	208569	8.0	0.01	191.29
□-125x125x**3.2A** (column, panel)	255.21	390.47	26.39	207157	5.0	0.02	300.40
□-125x125x**3.2B** (panel)	342.50	430.22	27.55	202740	2.5	0.01	315.65
□-125x125x**6** (column, panel)	403.32	493.27	21.67	208054	2.0	0.01	487.41
BH-150x125x**4.5**x6 (beam)	316.38	410.77	27.32	211200	—	—	—
BH-150x125x**6**x9 BH-150x125x4.5x**6** (beam)	306.85	402.72	28.63	208000	—	—	—
BH-150x125x6x**9** (beam)	252.10	397.27	31.88	207600	—	—	—

σ_y : yield stress
σ_u : tensile strength
ε: elongation
σ_c : compressive strength
E_s : elastic modulus of steel
E_{st} : modulus of strain hardening zone
ε_{st} : strain at stating point of strain hardening
ε_y : yield strain

2.5 Test Results

Figure 9 shows the relations between the horizontal load (H) and the column chord rotation angle ($R = \Delta/h$) of all specimens. The load and angle were taken positive when the horizontal jack pushed the base beam to the left. The solid and dotted or dash-dotted lines indicate the calculated elastic stiffness line and simple plastic mechanism line including $P\Delta$ effect, respectively. The mechanism line was based on a mechanism state with the plastic hinges forming at certain positions which are discussed in 2.5.2. The calculations of ultimate flexural strength of the

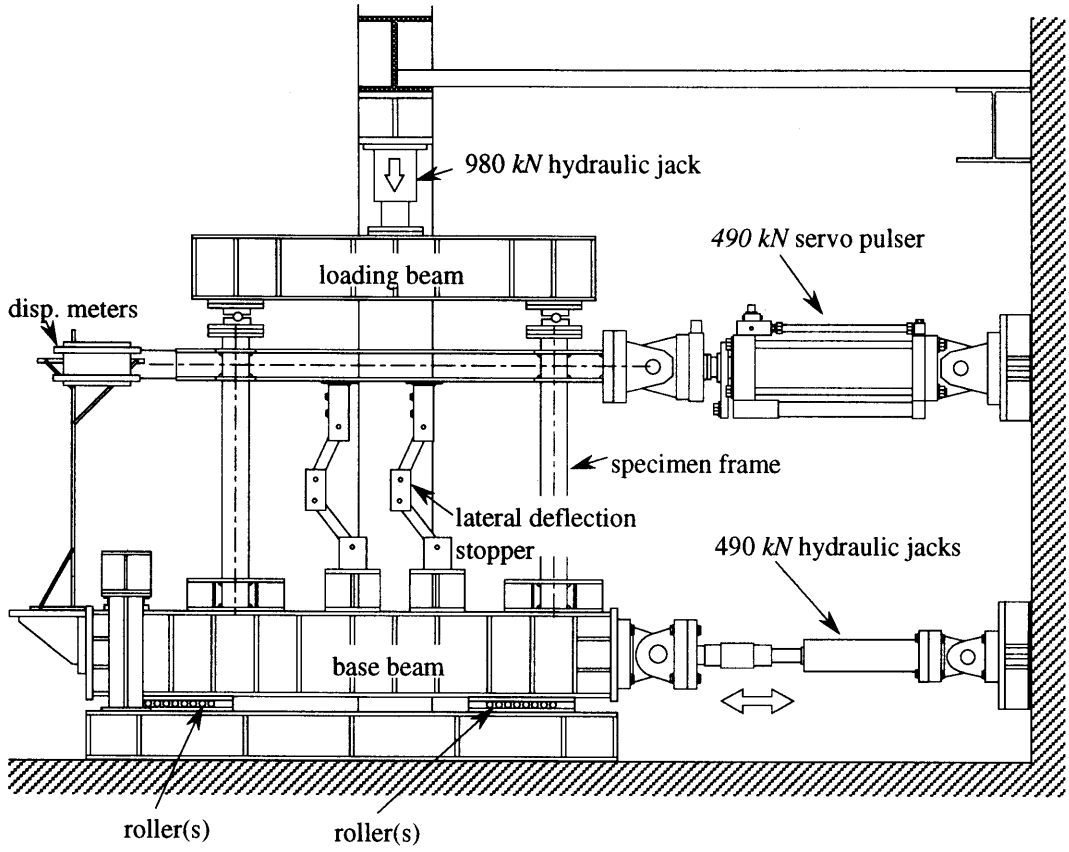

Fig. 5 Test setup

Table 4 Mixture of concrete

Gm	Sl	a	W/C	S/A	W	AE	C	S	G
[mm]	[cm]	[%]	[%]	[%]	[kg/m^3]	[kg/m^3]	[kg/m^3]	[kg/m^3]	[kg/m^3]
15	18	2	66	50	184	—	277	903	920

Gm : maximum dimension of coarse aggregate Sl : slump a : air content

W : water content per unit volume of concrete

AE : weight of air entraining agent per unit volume of concrete W/C : water-cement ratio

C : cement content per unit volume of concrete S/A : sand percentage

S : weight of fine aggregate per unit volume of concrete

G : weight of coarse aggregate per unit volume of concrete

Table 5 Mechanical properties of concrete

Specimen	F_c [N/mm^2]	E_c [N/mm^2]	age [days]	ε_u [%]
21SCC15	18.55	20022	43	0.02
21SCC30	17.82	20010	61	0.02
21SCP15	18.53	19626	49	0.02
21SCP30	18.79	20150	63	0.02
39SCC15	13.72	17218	137	0.02
39SCC30	15.91	18522	144	0.02
54SCC15	16.19	18693	146	0.02
54SCC30	20.82	21188	148	0.02

F_c : cylinder strength of concrete

Ec: elastic modulus of concrete

ε_u: yield strain

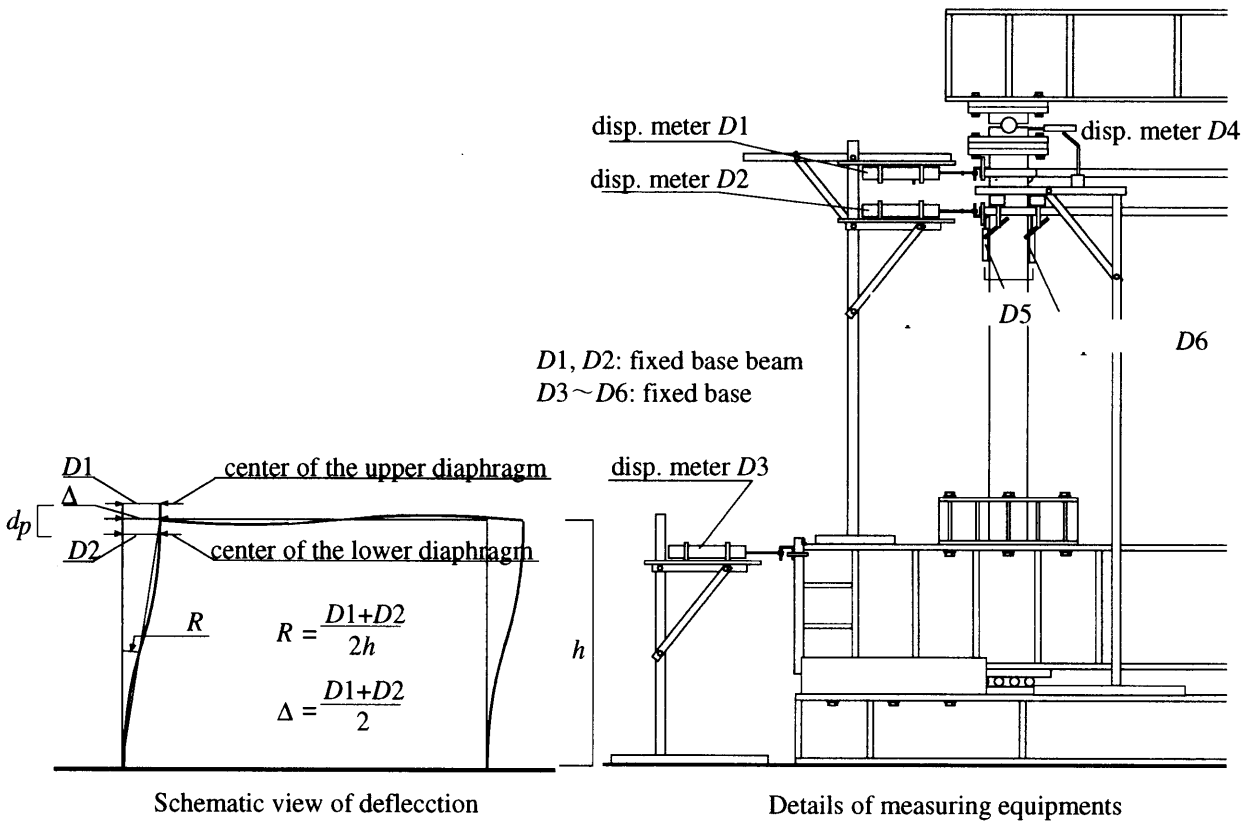

Fig. 6 Measuring equipments

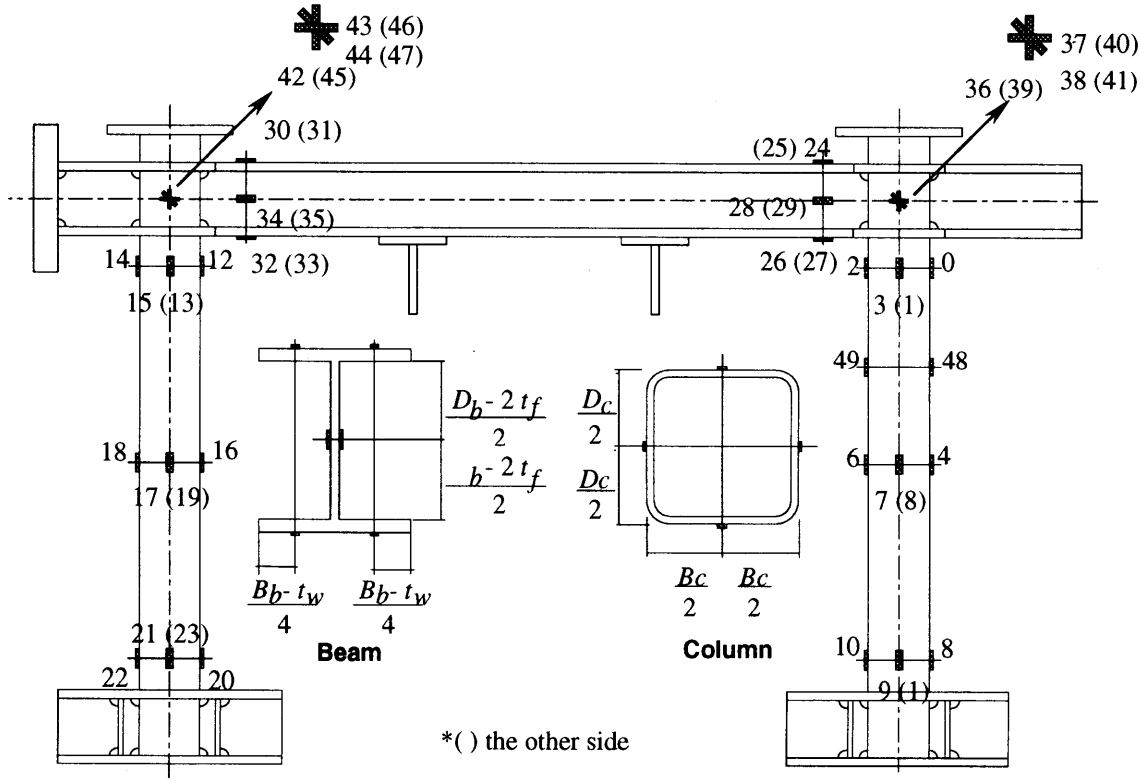

Fig. 7 Location of wire strain gauges (W.S.G.)

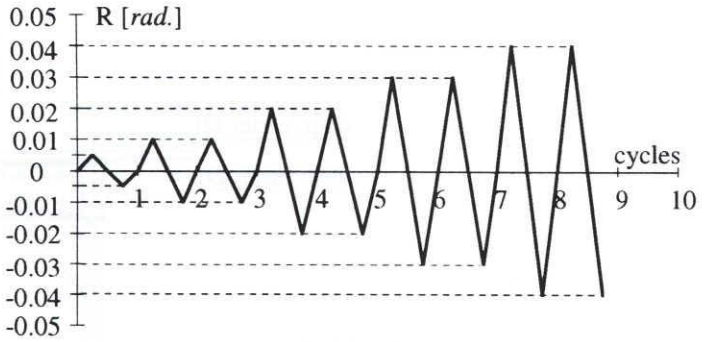

Fig. 8 Loading rule

column were based on the formulas specified in *AIJ Standard for SRC structures*[4], ignoring the effect of local buckling. The solid circles show the points at which local buckling of the column was observed, and the X marks show the point of the fracture or crack observed in the steel tube, which will be explained later in detail.

Figure 10 shows the load-strain relations, where ε-00, ε-08 and ε-38 indicate the strains measured by the strain gauges *No.* 0, 8 and 38 shown in Fig. 7.

2.5.1 Hysteretic behavior and failure modes

All specimens of column-yielding type showed the stable hysteresis loops. In the case of 21SCC15 and 21SCP15 which were subjected to smaller axial load with $D/t = 21$, the fracture at the welded part between the column tube and diaphragm plate occurred rather earlier, and caused the severe strength deterioration, because the fillet welding was used. This phenomena was observed only in these two specimens and not in the case of 21SCC30 and 21SCP30 which were subjected to the larger axial load. In specimens of $D/t = 39$ and 54, whose column tube and diaphragm plate were connected by butt welding, the fracture did not occur and the stable loops were obtained.

The hysteresis loops of the specimens subjected to smaller axial load with $D/t = 39$ and 54, *i.e.*, 39SCC15 and 54SCC15, showed a slightly pinched shape as seen in reinforced concrete columns. In these specimens, the tensile cracking occurred in concrete since the axial compression load was small, and the behavior of concrete is more pronounced since the amount of steel is small. These are the reasons why pinching behavior was observed. The crack of the steel tube was observed at the expanded portion due to local buckling in the specimen 54SCC15 at the amplitude equal to + 5/100 *rad.*, which was subjected to smaller axial load with the largest . However, this did not cause any severe strength deterioration.

The hysteresis loops of the specimens of panel-yielding type were also stable and spindle-shaped, although the fracture at the welded part similar to the one observed in the specimen 21SCC15 occurred again. The shape of the loop is quite similar to that of the corresponding specimen of column-yielding type, but it seems that Baushinger effect is just a little more pronounced in the specimens of panel-yielding type.

At the end of the test, the beams remained elastic. The strain data shown in Fig. 10 indicates that the connection panel of the specimens pf column-yielding type slightly yielded; the panel diagonal strain ε-38 remained within 0.5 %, except for the specimen 54SCC15 whose strain ε-38 reached about 1.5 %. The reason of the panel yielding of

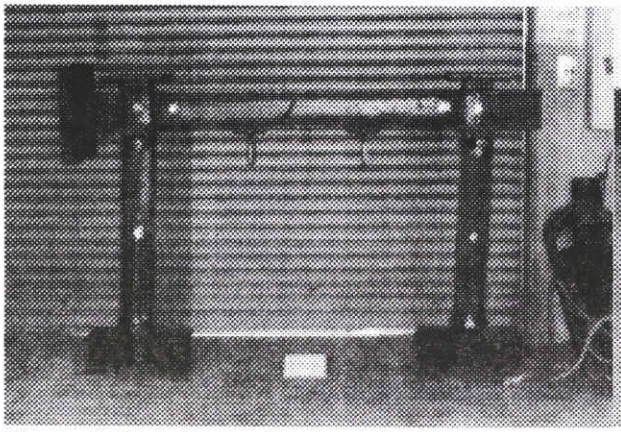

Photo 1 Specimen after test (54SCC30)

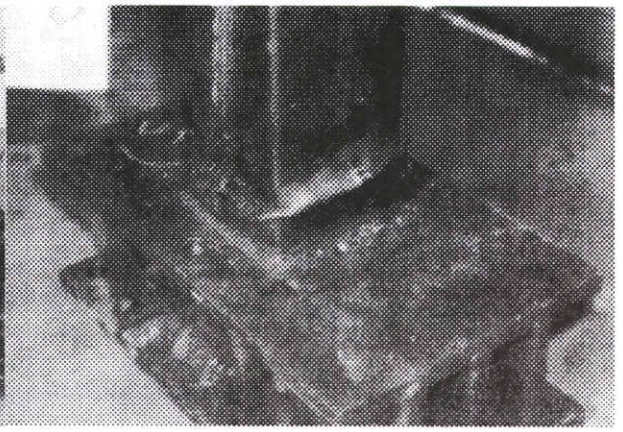

Photo 2 Local buckling at column tube (54SCC30)

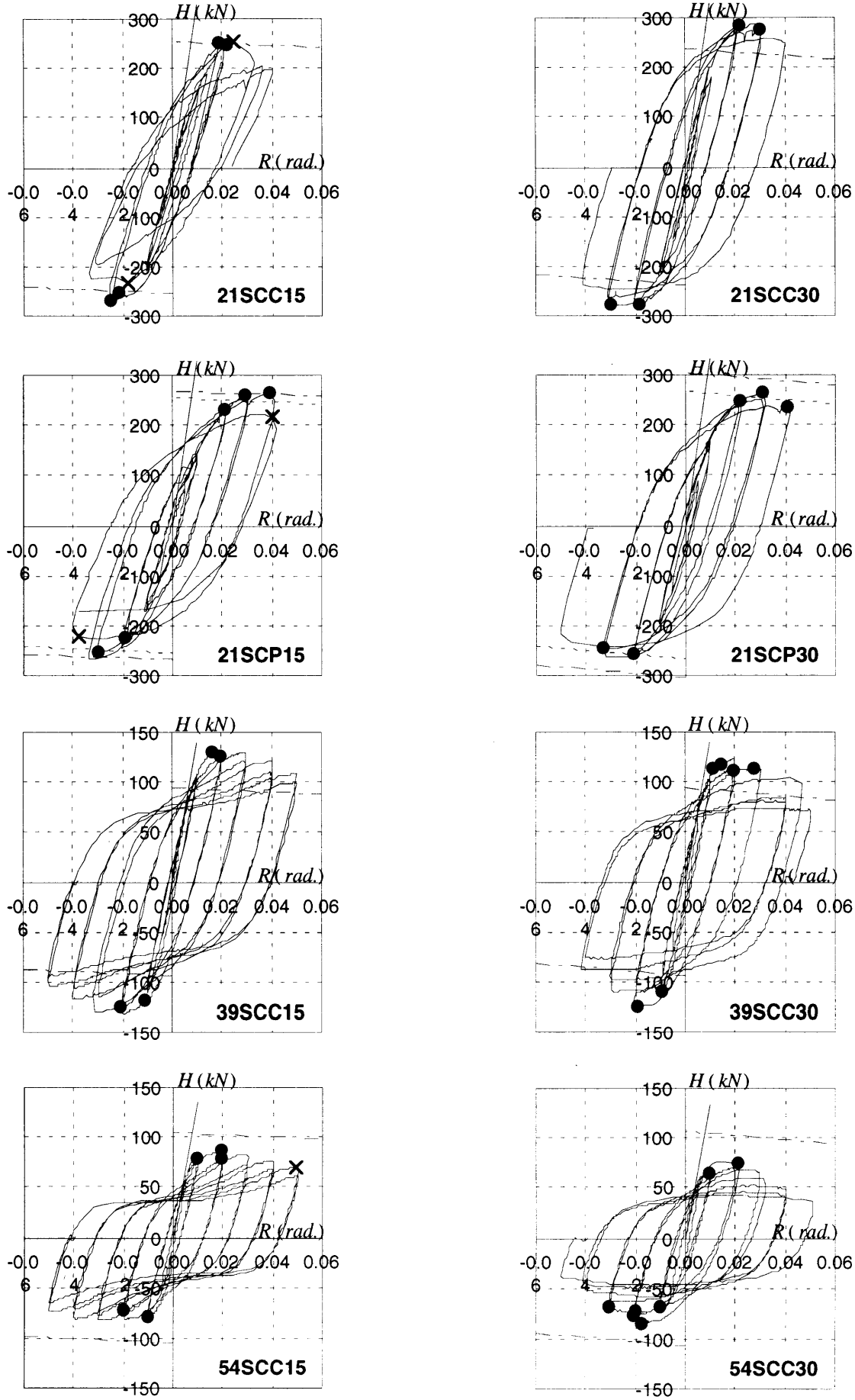

Fig. 9 H-R relations

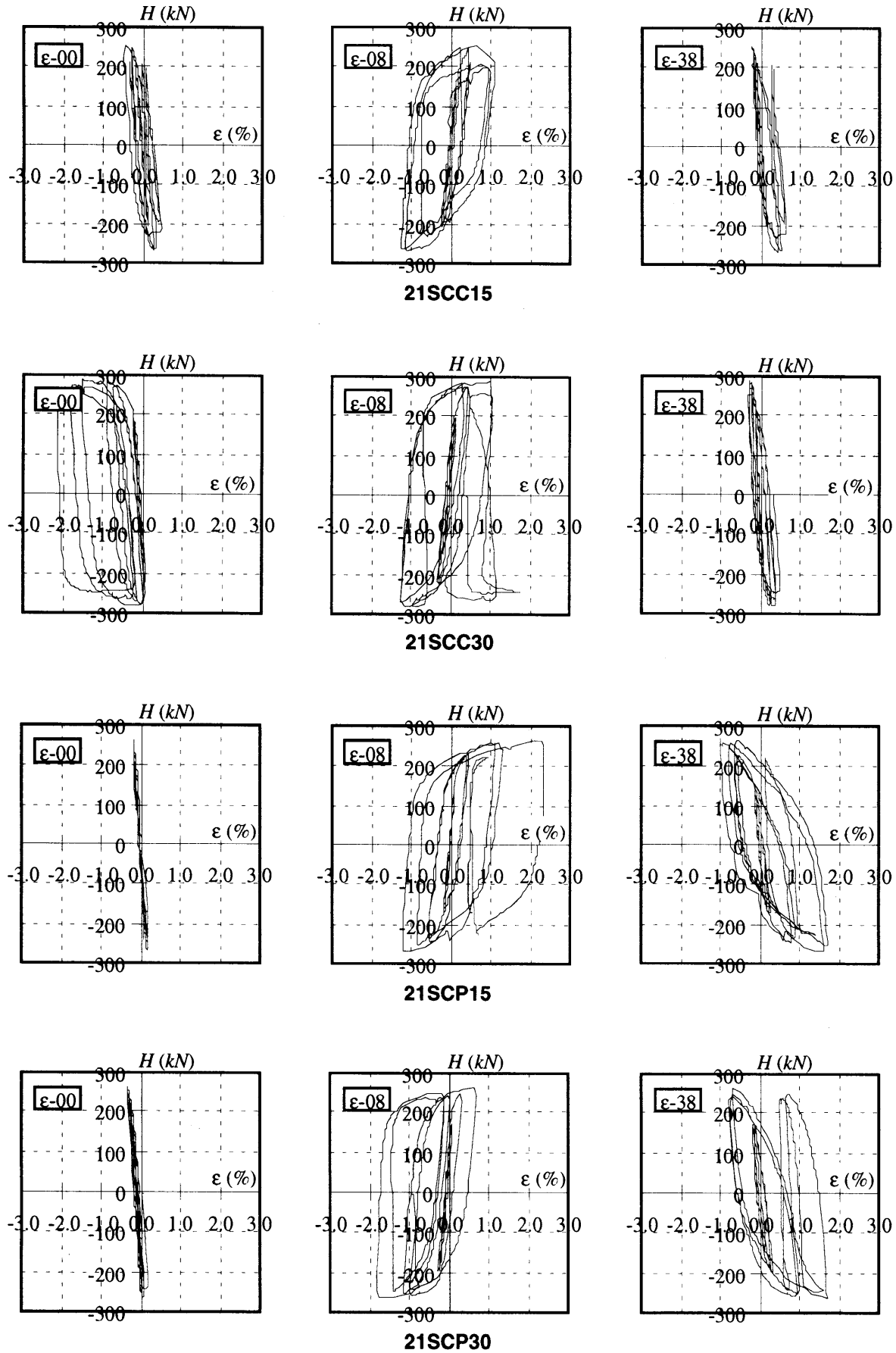

Fig. 10 H-ε relations

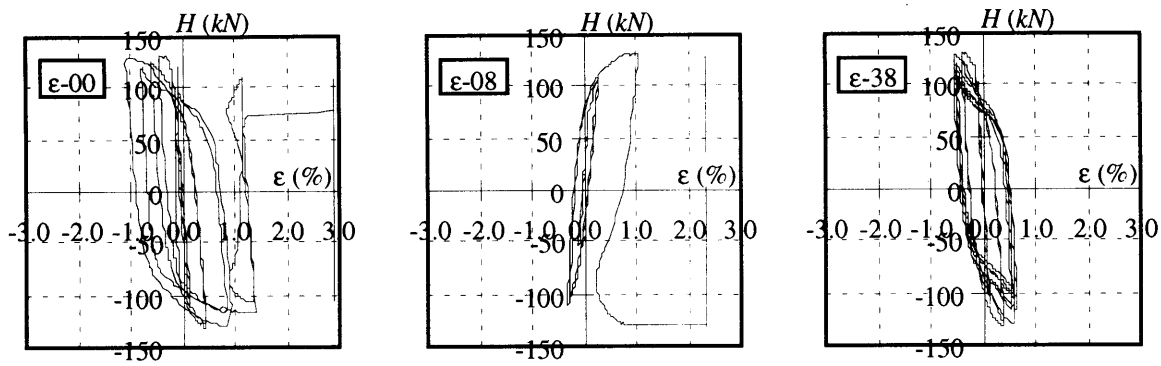

39SCC15

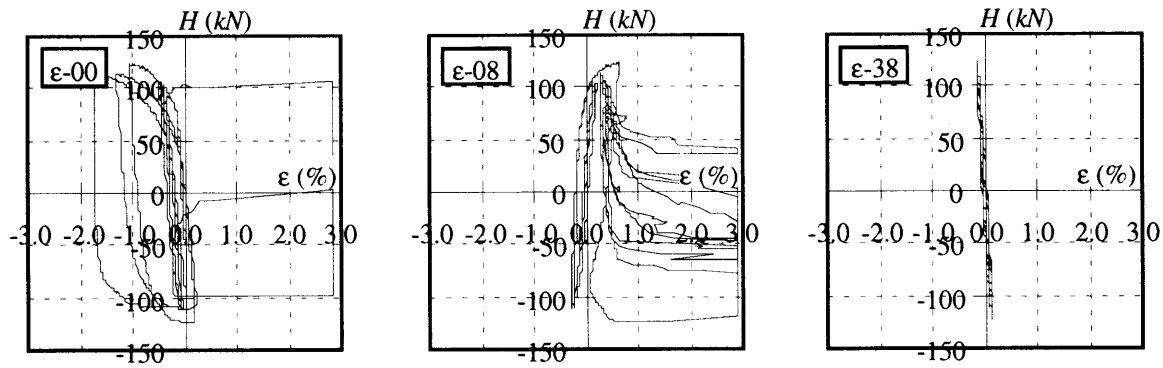

39SCC30

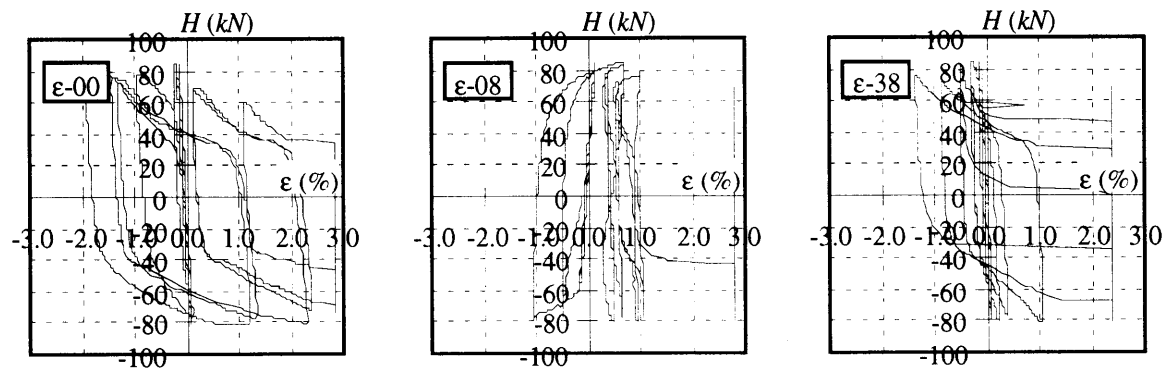

54SCC15

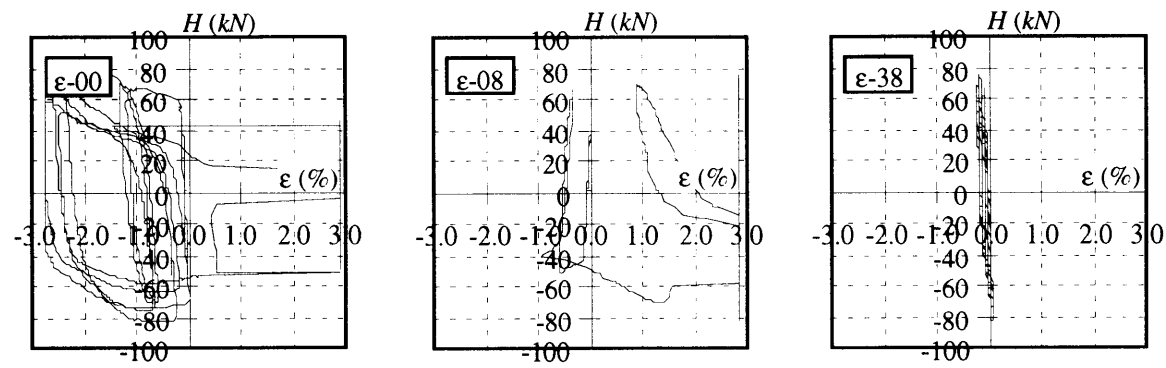

54SCC30

Fig. 10 H-ε relations (continued)

this specimen is not clear, since other diagonal strains ε-41, ε-44 and ε-47 (see Fig. 7) were less than 0.25%. In the case of the specimens of panel yielding type, 21SCP15 and 21SCP30, the panels (ε-38) and the lower end of the columns (ε-08) well yielded, and the top end of the columns (ε-00) remained elastic.

The local buckling was observed at the bottom part of the column first, and at the top part next in all specimens as shown in Photos 1 and 2.

2.5.2 Maximum strength

Rigid plastic collapse mechanism strength of the specimen of column-yielding type was calculated assuming that four plastic hinges with the full-plastic moment ${}_cM_U$ formed in two columns at the distance of half the width of the column tube parting from the surfaces of the beam and the column base stub, as shown in Fig. 11(a). The calculated collapse mechanism horizontal strength H_{cal} of the specimen of column-yielding type is then given by

$$H_{cal} = \frac{4M_U}{h - \frac{d_p}{2} - D_c} \tag{1}$$

On the other hand, in the case of the specimens of panel yielding type, it was assumed that the bending moment at the intersection of the center lines of the beam and column reached M_U at the mechanism state, as shown in Fig. 11(b), which is the bending moment generated when the connection panel fails in shear. Then, H_{cal} is given by

$$H_{cal} = \frac{2M_U + 2M_U}{h - \frac{D_c}{2}} \tag{2}$$

M_U is related to the bending moment in the beam M_B at the column surface as follows:

$$M_U = M_B \frac{\frac{l}{2}}{\frac{l}{2} - \frac{D_p}{2}} \tag{3}$$

The values of ${}_cM_U$ and M_B were calculated according to the formulas given in *AIJ Standard for SRC Structures*[4].

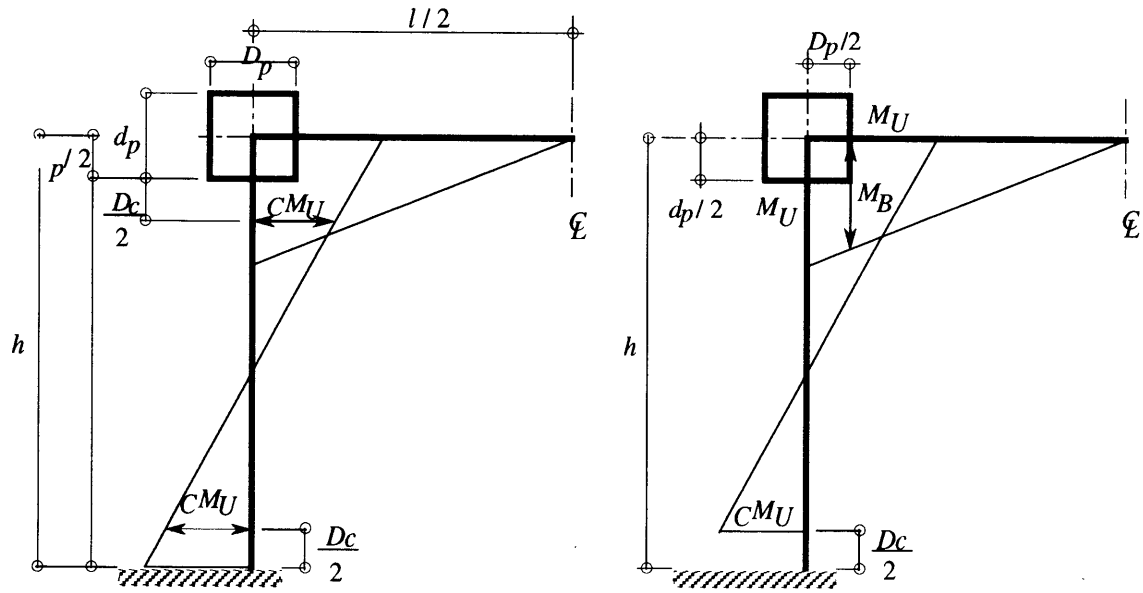

(a) column-failing **(b) connection-failing**

Fig. 11 Moment diagram

The mechanism lines shown by dash-dotted and dotted lines in Fig. 9 are drawn including the $P\Delta$ effect, based on the values of H_{cal} given by Eqs. (1) and (2), respectively. It is observed from Fig. 9 that the maximum strength of all specimens, except for the specimen 21SCC15 in which the fracture occurred in the early stage of loading and the specimens with $D/t = 54$, well exceeded the mechanism line even though the local buckling occurred, because of the strain hardening of steel. In the case of the specimen 21SCC30, the strength deterioration due to the local buckling is rather larger, since the percentage of the strength provided by the steel tube to the total strength is higher than other specimens with larger ratio, and the restraining of concrete on the growth of the local buckling deformation is not so effective. The maximum strength of the specimens with $D/t = 54$ could not reach the mechanism line, because of the strength reduction due to local buckling, but the strength deterioration after the local buckling was

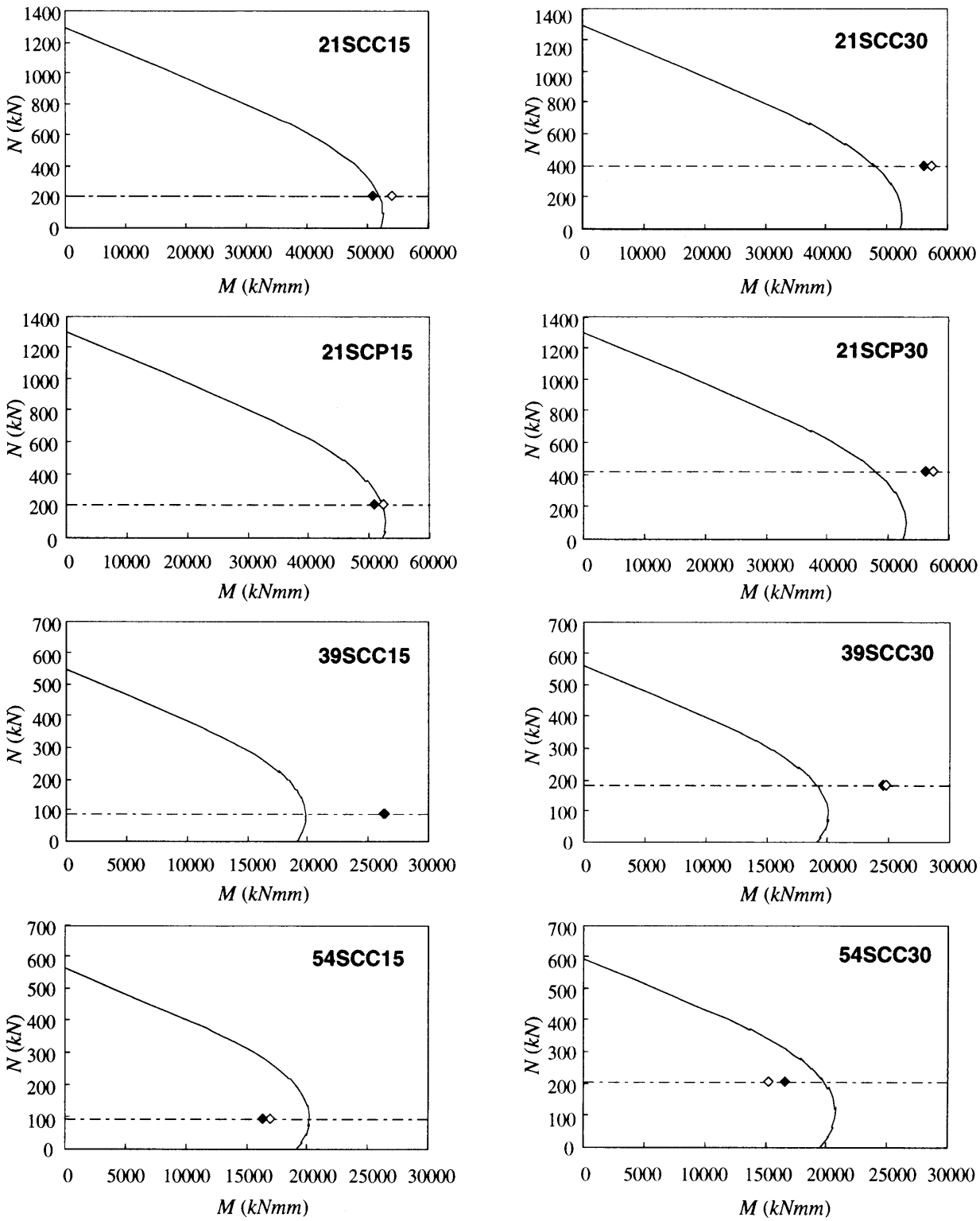

Fig. 12 N-M interaction curves

not so large due to the restraining effect of concrete on the growth of local buckling deformation.

It is quite interesting to note that the strength of the specimens of panel-failing type, 21SCP15 and 21SCP30, exceeded the mechanism line calculated on the basis of the ultimate shear strength of the connection panel, and reached or even exceeded the mechanism lines based on the collapse mechanism in which four plastic hinges formed at both ends of two columns. This is mainly due to the strain-hardening of the panel tube and the strength rise in the panel concrete which was highly confined by the steel tubes and beam flange and web.

Figure 12 shows the ultimate strength interaction curves between the axial force N and the bending moment M, calculated for the columns of all specimens according to the procedure shown in *Ref. 5)*, ignoring the effect of local buckling. The plots marked by solid and open squares indicate the flexural strengths of the column deduced from the strengths of the frame specimen detected in the positive and negative loading sides, respectively, where the column strength was deduced by substituting the maximum horizontal strength obtained in the tests into H_{cal} in Eq. (1) and solving it for ${}_CM_U$. The same treatment was taken for the specimens of panel-yielding type, since their strengths also reached the mechanism lines calculated based on the column strength. The strengths of 21SCC15 and 21SCP15 were just on the interaction curve, since the fracture occurred, otherwise their strengths may have well exceeded the interaction curve, as observed in the case of other specimens with D/t = 21 and 39. The difference between the strength deduced from the test results and those given by the interaction curves is larger in the specimens with D/t = 39 than in the specimens with D/t = 21, and thus it may be said that the effects of filled-concrete was more pronounced in the former. In the case of the specimens with D/t = 54, the strengths were much smaller than those given by the interaction curves, due to the local buckling.

3. Discussions

The D_S factor is a factor used in the seismic design practice in Japan, and equivalent to R_W factor in the U.S. and *q-factor* in Europe. This is to determine the required horizontal strength of the frame under a very severe seismic loading, and is related to the ductility of the frame. According to the *Building Standard Law of Japan*[6], the design horizontal load of the elastic frame must be taken equal to the vertical load W, that is, the shear coefficient Q/W is set equal to unity. On the other hand, the required horizontal strength for the ductile frame can be reduced to $Q = D_S W$ according to the ductility of the frame. This reduction factor D_S is called structural characteristic factor, and is expressed by using the plastic deformation capacity (μ) as follows:

$$D_s = \sqrt{\frac{1}{1+2\mu}} \qquad (4)$$

In the case of monotonic loading, the value of the plastic deformation capacity m is often calculated in reference to the horizontal displacement of the frame at the maximum strength or at the strength reduced to 90 % of the maximum strength. However, in the case of the cyclic loading as shown in Fig. 13 (a), equivalent plastic deformation capacity must be derived. *Kato*[7] showed that the monotonic load-deformation curve of a CFT member can be approximated by a curve which envelopes a series of curves obtained by connecting the positive half of the hysteresis loop in each cycle of loading as shown in Fig. 13 (b). In the present derivation of m, a series of curves similar to those shown in Fig. 13 (b) are prepared from the test data. Then, the bilinear load-deformation relation of the ideal elastic-perfectly plastic type is composed in such a way that the area S covered by this relation shown in Fig. 13 (c) is equal to the total sum of the areas S covered by each positive half of the hysteresis loop shown in Fig. 13 (b), which is defined as the area within 90% of the maximum strength. The ultimate strength H_{cal} of the ideal relation shown in Fig. 13 (c) is the rigid plastic collapse mechanism strength based on the mechanism state with four plastic hinges forming in columns. The same treatment was taken for the specimens of panel-yielding type, since their strengths also reached the mechanism lines calculated based on the collapse mechanism with four plastic hinges forming in columns. Finally, the equivalent plastic deformation capacity μ is calculated as $\mu = R_u / R_y - 1$, as shown in Fig. 13 (c).

A question often arises whether or not D_S factor should be calculated from the load-deflection curve shown in Fig. 13 (a) and (b) in which the load H includes the reduction by $P\Delta$ effect. In order to check this point, another set of D_S factor was calculated from the relation between H' and R, where $H' = H + P\Delta$, P being the total vertical load on the frame.

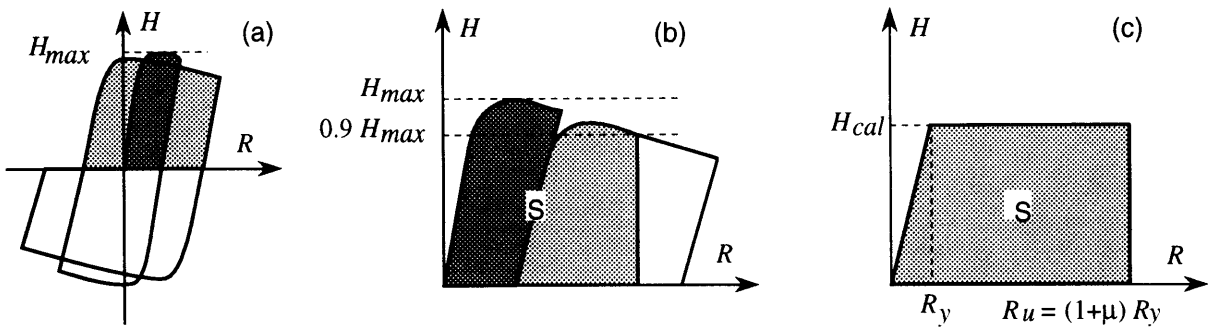

Fig. 13 Equivalent plastic deformation capacity

The values of D_s calculated by the method explained above are plotted against the values of D/t in Fig. 14 (a), where the solid horizontal lines indicate the relations specified by *BCJ Requirements*[3] for pure steel frames. The number shown at each plot is derived from H'-R relation, and the number in the parenthesis from H-R relation, the latter including the reduction of the horizontal load due to $P\Delta$ effect. It is observed from Fig. 14 (a) that the values of D_s of CFT frames are much smaller than those specified for the pure steel frames, and thus the earthquake resistant capacity of CFT frame is quite high, except for 21SCC15 in which the fracture at the welding occurred. The difference between the value of D_s obtained for the CFT frame and that specified for the steel frame becomes the largest in the specimens with $D/t = 39$. As explained before, the strength deterioration after the local buckling was rather large in the specimen with $D/t = 21$, and the maximum strength was reduced by the local buckling in the specimens with $D/t = 54$. Therefore, the filled-concrete is most effectively utilized in the specimens with $D/t = 39$. Comparison of the values of D_s calculated by taking out the $P\Delta$ effect with those including $P\Delta$ effect shows that the former is a little smaller, and the difference is small since CFT columns of the tested frames were stocky. The difference becomes larger in the specimens with the axial load ratio equal to 0.3. The value of D_s of the specimen of panel-yielding type is slightly larger than that of the corresponding specimen of column-yielding type. This is because the area S in Fig. 13 (c) was evaluated using the value of H_{cal} determined by Eq. (1), *i.e.*, based on the collapse mechanism with four plastic hinges forming in columns. If the value of H_{cal} determined by Eq. (2) which was for the panel-yielding mechanism was used, the value of D_s would be much lower than the present value.

The values of D_s shown in Fig. 14 (b) are obtained from the envelop curve of H'-R relation, as often done in the evaluation of the deformation capacity of reinforced concrete members, and they are higher than the corresponding values in Fig. 14 (a). Thus, the value of D_s based on the cumulative plastic deformation is smaller than that based on the envelope curve. This comparison clearly shows that the value of D_s highly depends on the loading history and the number of loading cycles. The most suitable loading history taken in the test to evaluate D_s still remains in question. This problem must be discussed in relation to the dynamic response analysis using the realistic restoring-force characteristics. The reason why the value of D_s of 21SCC30 exceeds the value for the pure steel frame is that the strength deterioration after the local buckling was large in this specimen, as mentioned before.

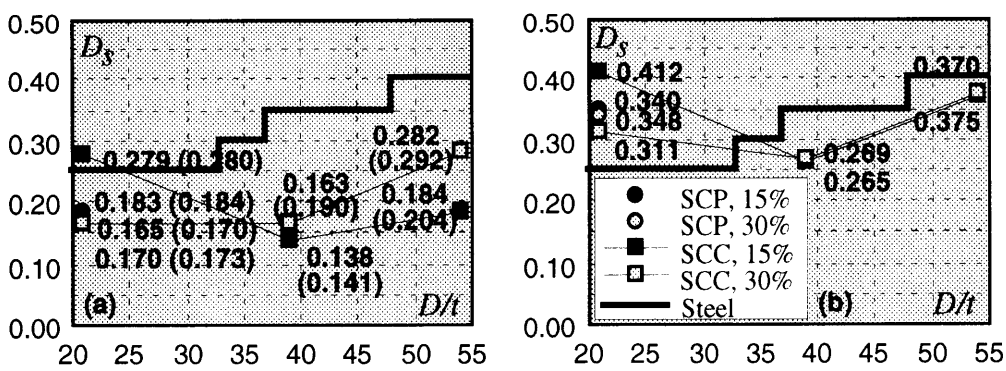

Fig. 14 Ds Factor

The effect of the beam remaining elastic is not clear since the data of the frame in which both steel beam and CFT column yield are not available. However, it could be at least concluded that the performance of the frame with inelastic steel beam and CFT column would be still better than the pure steel frame, if the beam is properly proportioned against lateral buckling and local buckling.

4. Conclusions

From the cyclic loading test of frames consisting of CFT columns, the following observations were made.

1) In two of the specimens subjected to the smaller vertical load, the fracture occurred in the welded part at the column end, because the fillet welding was accidentally used. It caused serious strength reduction.
2) All specimens except those having failed in the fracture showed fairly stable hysteresis loops, although the local buckling occurred in the steel tube. In the case of the specimens with $D/t = 54$, the behavior of concrete was more pronounced since the amount of steel was small, and the hysteresis loops were a little pinched. It seems that Baushinger effect is a little more pronounced in the specimen of panel-yielding type than in the corresponding specimen of column-yielding type.
3) The maximum strength of all specimens, except for the specimen 21SCC15 in which the fracture occurred in the early stage of loading and the specimens with $D/t = 54$, well exceeded the mechanism line even though the local buckling occurred, because of the strain hardening of steel. The maximum strength of the specimens with $D/t = 54$ could not reach the mechanism line, due to the strength reduction caused by local buckling.
4) The maximum strength of the specimens of panel-failing type exceeded the mechnism line calculated on the basis of the ultimate shear strength of the connection panel, and reached or even exceeded the mechanism line based on the collapse mechanism in which four plastic hinges formed at both ends of two columns. This is mainly due to the strain-hardening of the panel tube and the strength rise in the panel concrete which was highly confined by the steel tubes and beam flange and web.
5) The strength deterioration after the local buckling is rather large in the case of the specimen with $D/t = 21$, since the large percentage of the strength was provided by the steel tube, and the restraining effect of concrete on the growth of the local buckling deformation was not much expected. On the other hand, in the case of the specimen with $D/t = 54$, the strength deterioration was small since the concrete's restraining was effective.
6) The values of D_s derived from the test data highly depend on the loading history and the number of loading cycles. Those obtained from the cumulative plastic deformation capacity were quite smaller than the values used for the pure steel frame in real practice, and the maximum difference was observed in the specimen with $D/t = 39$.

Acknowledgments

The research work presented in this paper was supported by the *Grant-In-Aid for Scientific Research* (B) (*No.* 08455253 Principal Investigator: Shosuke Morino) granted by the Ministry of Education, Japan.

References

1) Matsui, C. : *Strength and Deformation Capacity of Frames Composed of Wide Flange Beams and Concrete Filled Square Tubular Columns*, Proceedings of Pacific Structural Steel Conference, Vol. 2, pp. 169-181, 1986.
2) Morino, S., Kawaguchi, J., Yasuzaki, C. and Kanazawa, S. : *Behavior of Concrete-Filled Steel Tubular Three-Dimensional Subassemblages*, Proceedings of Engineering Foundation Conference on Composite Construction in Steel and Concrete II, pp. 726-741, 1992.
3) *Structural Requirements for Building Construction*, The Building Center of Japan, 1994.
4) *AIJ Standard for Structural Calculation of Steel Reinforced Concrete Structures*, Architectural Institute of Japan, 1987.
5) Kawaguchi, J. and Morino, S. : *Ultimate Strength Interaction of Steel-Concrete Composite Sections under Biaxial Bending (part 1)*, Summaries of Technical Papers of Annual Meeting, Vol. C, Architectural Institute of Japan, pp. 1731-1732, 1992.8.
6) *The Building Standard Law of Japan*, The Building Center of Japan, 1986.
7) Kato, B. : *Strength and Rotation Capacity of Concrete-Filled Steel Tubular Columns under Combined Compression and Bending (Strength and rotation capacity of concrete-filled tubular columns, Part II)*, Journal of Structural and Construction Engineering (Transactions of AIJ), No. 486, pp. 157-166, 1995.11.